

## Supporting Information

### Macroporous C@MoS<sub>2</sub> composite as anode for high-performance sodium-ion batteries

Yan Yang <sup>+, a, \*</sup>, Lei Wang<sup>+, a, b</sup>, Cong Suo<sup>a</sup>, and Yining Liu <sup>a, b</sup>

<sup>a</sup> SINOPEC (Dalian) Research Institute of Petroleum and Petrochemicals Co., Ltd

<sup>b</sup> Institute of Environmental Remediation, Dalian Maritime University, Dalian 116026, P. R. China.

<sup>+</sup> These authors contributed equally to this work.

\*Corresponding authors.

E-mail address: yangyan.fshy@sinopec.com

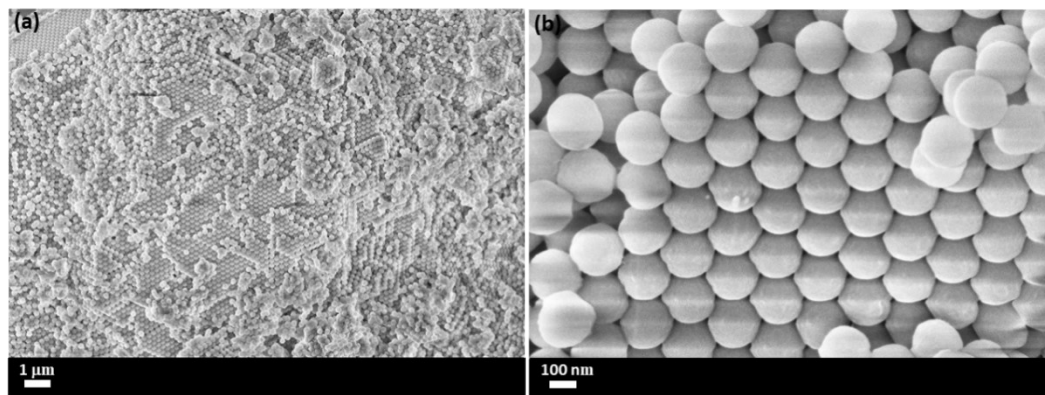


**Fig. S1.** SEM images of PS nanospheres with ordered 3D structure (a-b).

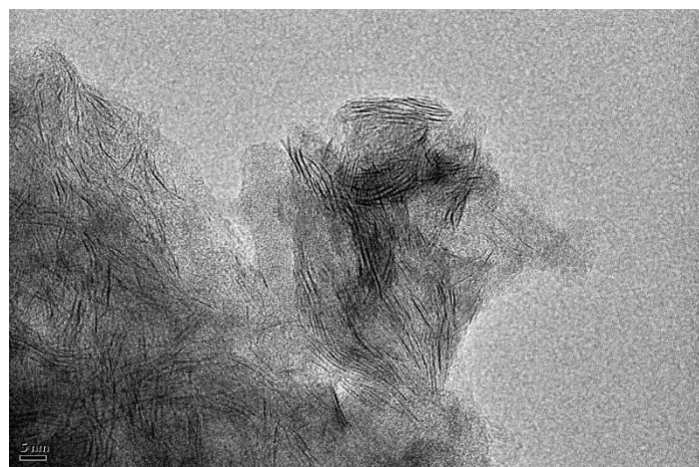


**Fig. S2.** Structure characterization of Porous C@MoS<sub>2</sub>, HRTEM image.

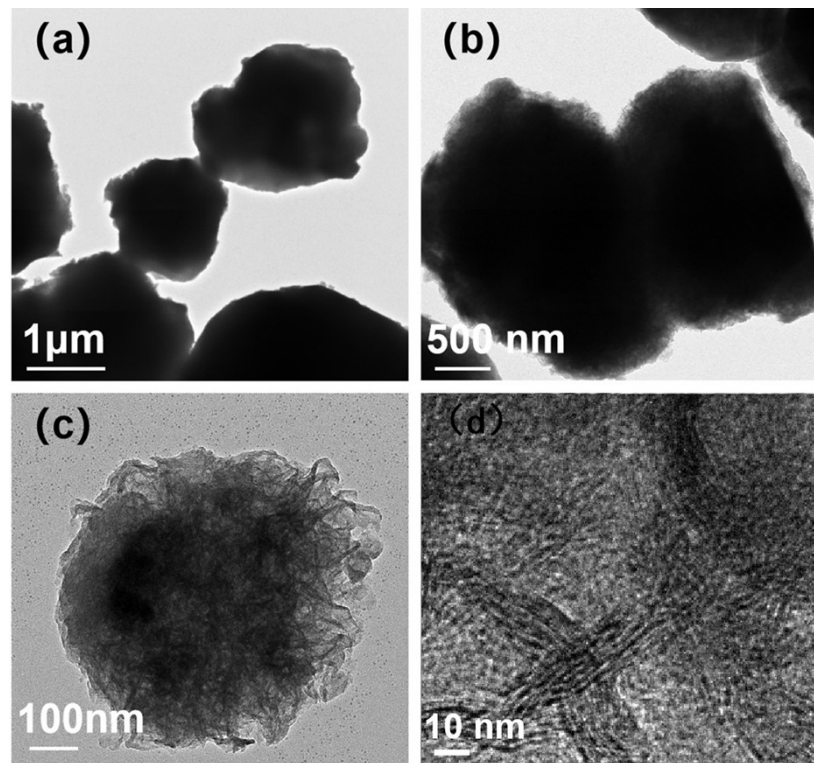


**Fig. S3.** The nanostructure characterizations of C@MoS<sub>2</sub>, TEM images (a-c) and HRTEM image (d).

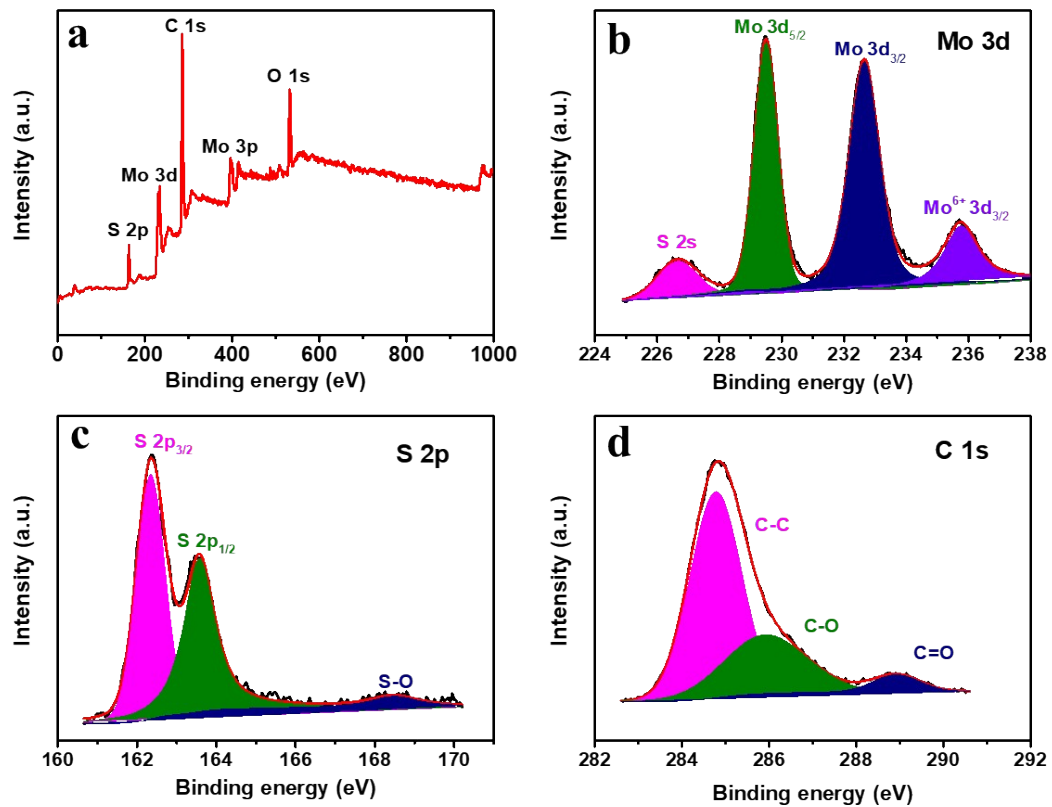


**Fig. S4.** Composition characterization of Porous C@MoS<sub>2</sub>. XPS survey spectrum of C@MoS<sub>2</sub> (a) and high-resolution XPS spectra of Mo 3d (b), S 2p (c), C 1s (d).

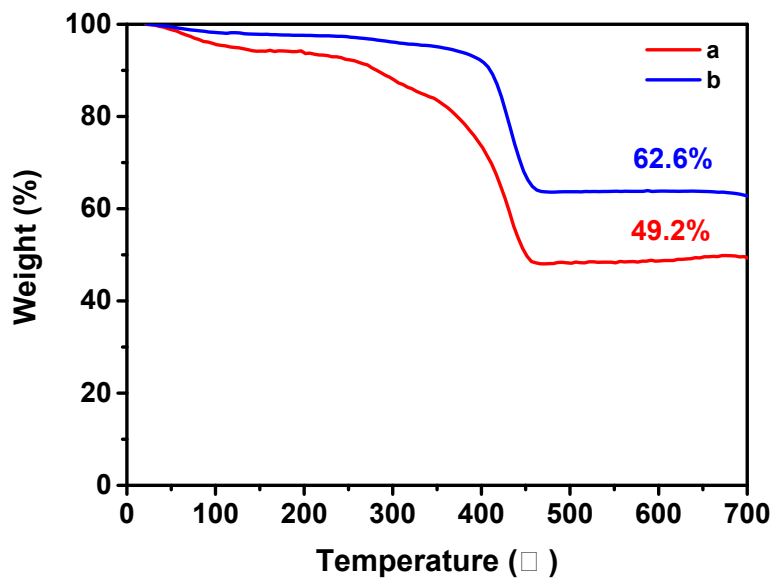


**Fig. S5.** TGA curves of Porous C@MoS<sub>2</sub> (a) and C@MoS<sub>2</sub> (b) in air at a heating rate of 10 °C min<sup>-1</sup>.

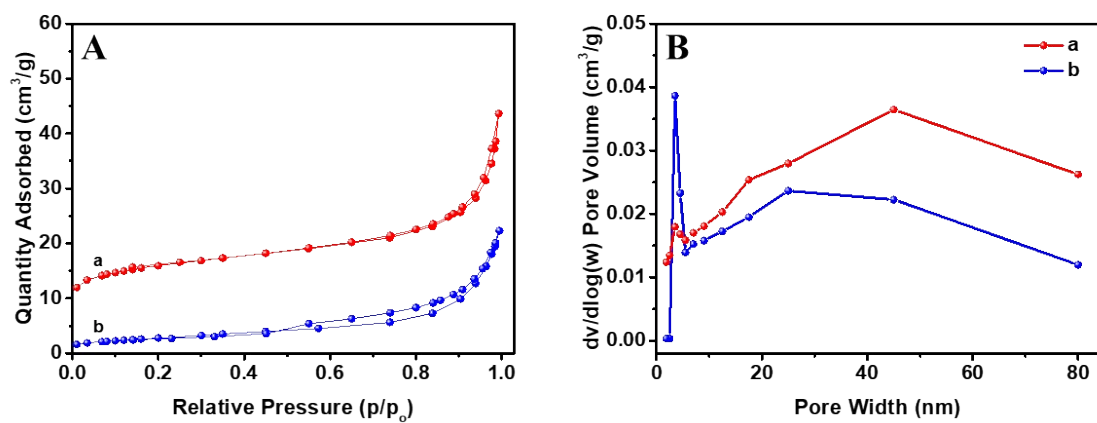


**Fig. S6** (A) The nitrogen adsorption-desorption isotherms and (B) pore size distribution plots of Porous C@MoS<sub>2</sub> (a) and C@MoS<sub>2</sub> (b).

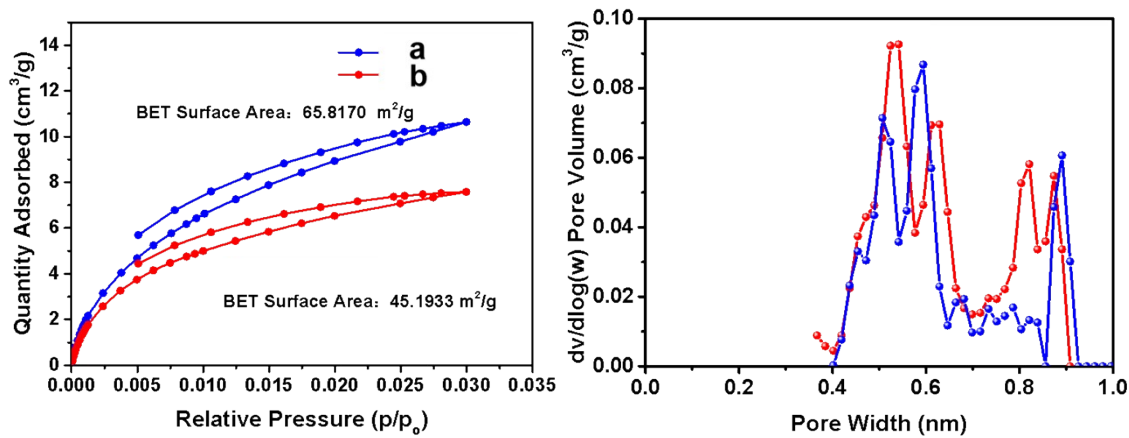


**Fig. S7.** (A) The CO<sub>2</sub> adsorption-desorption isotherms and (B) pore size distribution plots of Porous C@MoS<sub>2</sub> (a, blue line) and C@MoS<sub>2</sub> (b, red line).

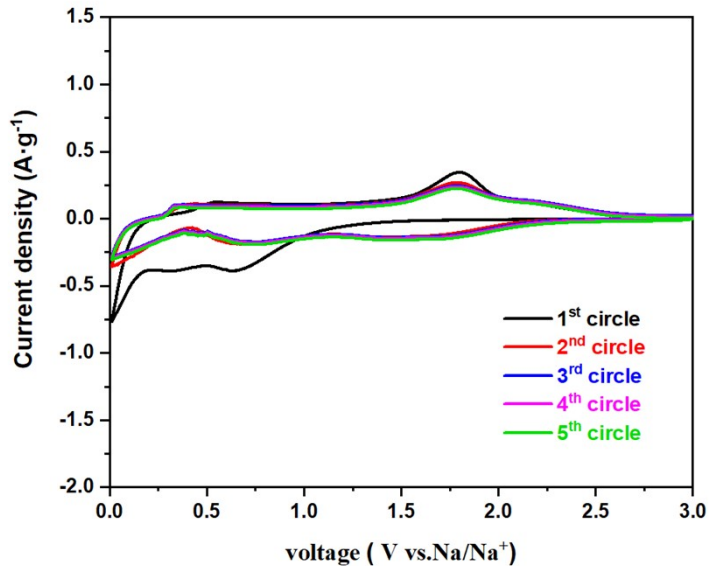


**Fig. S8.** CV curves of control sample C@MoS<sub>2</sub> for the first five cycles at a scan rate of 0.5 mV s<sup>-1</sup>.

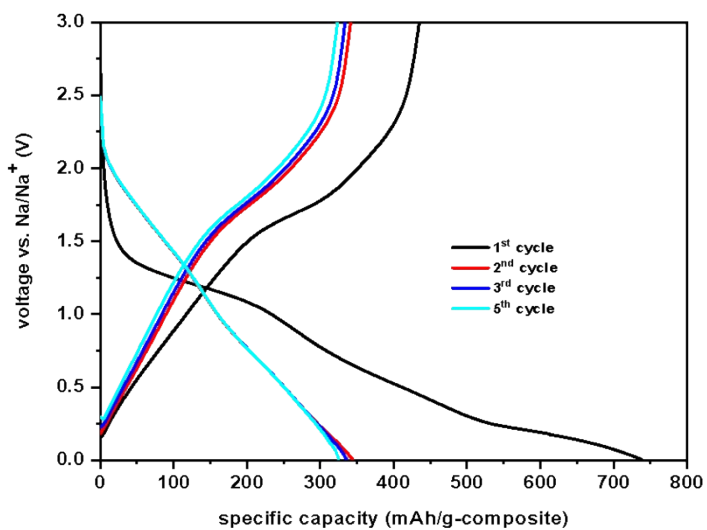


**Fig. S9.** The galvanostatic discharge-charge curves of C@MoS<sub>2</sub> at 500 mA g<sup>-1</sup>.

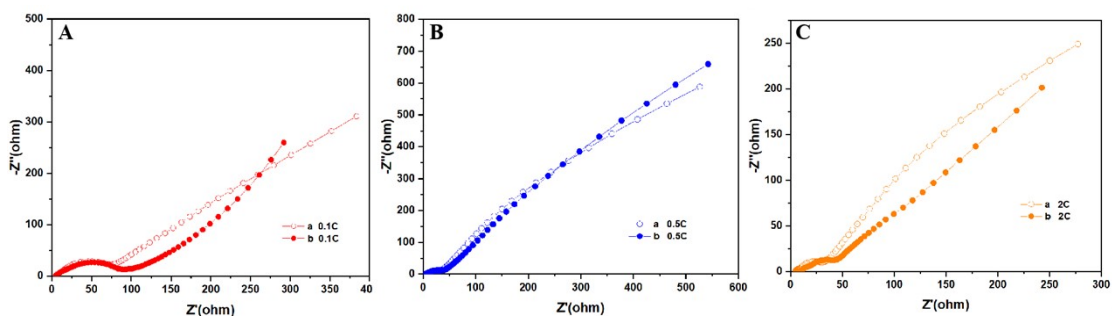


**Fig. S10.** EIS Nyquist plots of Porous C@MoS<sub>2</sub> (a) and C@MoS<sub>2</sub> (b) after 5 cycles at 0.1 C (A), 0.5C (B) and 2C (C) respectively.

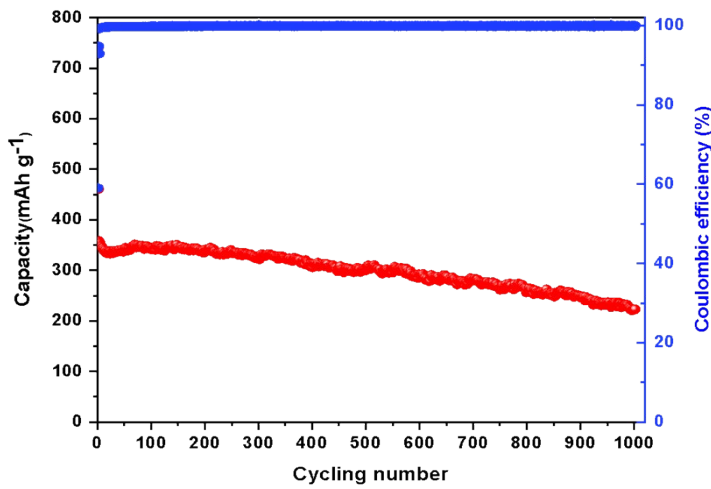


**Fig. S11.** Long-term cycling property and Coulombic efficiency of C@MoS<sub>2</sub> at a current density of 1000 mA g<sup>-1</sup>.

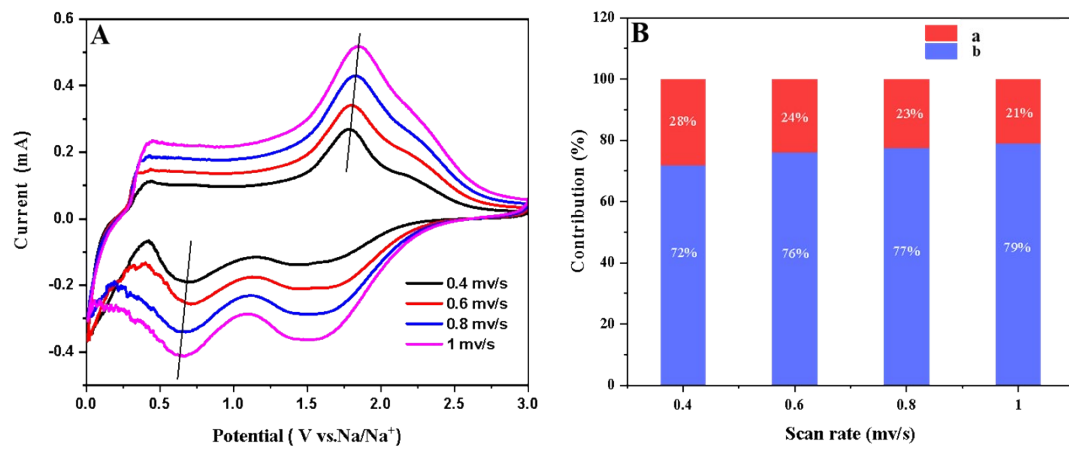


**Fig. S12.** (A) CV curves of Porous C@MoS<sub>2</sub> with different scan rates. (B) The contributions of the diffusion and capacitive-controlled storage at different scan rates of C@MoS<sub>2</sub>.

**Table S1.** The electrochemical performance comparasion of Porous Porous C@MoS<sub>2</sub> composites with other C/MoS<sub>2</sub>-based materials reported in the literature.

MoS <sub>2</sub> -base electrodes	Current (mA.g <sup>-1</sup> )	Cycles	Capacity (mA.h.g <sup>-1</sup> )	References
1T MoS <sub>2</sub> -graphene	50	200	313	[1]
MoS <sub>2</sub> -1-nm-TiO <sub>2</sub>	500	200	182	[2]
MoS <sub>2</sub> @C	80	100	184	[3]
1T-MoS <sub>2</sub> /CC	200	200	576	[4]
HC@MoS <sub>2</sub> @NC	100	100	321	[5]
WS <sub>2</sub> -MoS <sub>2</sub> -BioC	100	100	362.5	[6]
V-MoS <sub>2</sub> @CC	1000	100	311.2	[7]
Porous C@MoS <sub>2</sub>	1000	400	410	This work

1. X. Geng, Y. Jiao, Y. Han, A. Mukhopadhyay, L. Yang and H. Zhu, *Adv. Funct. Mater.*, 27 (2017) 1702998.
2. W. Ren, W. Zhou, H. Zhang and C. Cheng, *ACS Appl. Mater. Interfaces*, 9 (2017) 487-495.
3. X. Xie, T. Makaryan, M. Zhao, K. L. Van Aken, Y. Gogotsi and G. Wang, *Adv. Energy Mater.*, 6 (2016) 1502161.
4. W. J. Tang, X. l. Wang, D. Xie, X. h. Xia, C. d. Gu and J. p. Tu, *J. Mater. Chem. A*, 6 (2018) 18318.
5. Guoquan Suo, Baoguo Zhao , Rongrong Mu , Chuanjin Lin , Shazam Javed , Xiaojiang Hou , Xiaohui Ye , Yanling Yang , Li Zhang, *J. Energy Storage*, 77 (2024) 109801.
6. Jiantao Wang, Chongxia Zhong, Qixin Yang, Jinsong Li, *Appl. Surf. Sci.* 683 (2025) 161843.
7. L. N. Wang, X. Wu, F. T. Wang, X. Chen, J. Xu and K. J. Huang, *J. Colloid Interface Sci.*, 583 (2021) 579.